Measurements of sea-floor backscattering strength of very low frequency acoustic waves in western Mediterranean Sea; a comparison to GABIM [1]

Iannis Bennaceur[1], Nathan Ivkovic[1], Xavier Cristol[1], Adrien Rondeau[1], and Benoit Theckes[1]

[1]Thales Defence Mission Systems, FRANCE

Iannis Bennaceur, 525 route des dolines, 06560 Valbonne, FRANCE
iannis.bennaceur@fr.thalesgroup.com, +33492963291

Abstract: *In the context of anti-submarine warfare, active sonar performances depend on the amount of reverberated energy reaching the receiver after the powerful emission from the source. In the Very Low Frequency (VLF) range, the scattering by the sea-floor provides the largest contribution to the reverberation level that THALES DMS tries to better predict. An at-sea trial took place in the Mediterranean Sea in September* 2024*,* 30 *km off French Riviera coast in a deep-water environment. Two boats were involved, one carrying an acoustic source emitting at* 215 *Hz, immersed at* ≈ 7 *m under the sea-surface, the other conveying a vertical line array composed of* 13 *hydrophones spaced by* 3 *m. The center of the antenna was* 45 *meters below the sea-surface. The boats were spaced from few dozen meters, and* 1*-second Continuous Waves (CW) were transmitted in order to measure the acoustic Reverberated Level (RL) in this quasi-monostatic configuration. The output of classical weighted beamforming according to time and elevation angle allowed to extract RL according to the grazing angle* θ *in a range between* 25 *and* $65°$*. The evolution of the backscattering strength* σ*, deduced from RL, regarding* θ *is in good qualitative agreement with other measures that also took place in the Mediterranean Sea [2], where a strong decrease appears from* $\theta \approx 33°$*. However, our implementation of GABIM [1], ran with a first-guess geoacoustic model for the sea-floor, indicates that scattering from the volume inhomogeneities is the main contribution to backscattering strength, regardless of* θ*. This observation differs from the one made in [2] where scattering by the rough interface between sediments and the harder basement was the main contribution for intermediate grazing angles.*

Keywords: *Sea-floor reverberation, backscattering strength, very low frequency, GABIM*

1. ENVIRONMENT AND REVERBERATED LEVEL

During the trial (see abstract for details), the water temperature from the sea-surface to a depth of $750\,\mathrm{m}$ was measured using a XBT probe. The resulting celerity profile, extended to the water height ($H_w \approx 2388\,\mathrm{m}$) and displayed on the left part of Fig. 1, exhibits a strong thermocline. To construct a geoacoustic model for the sea-floor (right part of Fig. 1), needed for the σ computation, sites 371 and 374 from the Deep Sea Drilling Project were considered (site 372 was excluded because it took place over a rise). The Plio-Quaternary (P-Q) sediment thicknesses estimated from the Seanoe [3] and an in-house databases were found in agreement with the observations of the DSDP, which gave us confidence about using those databases to infer the sediment thickness at the experiment location. A 800-m thick P-Q sediment layer was estimated, that we decided to split into 2 parts; an unconsolidated layer of marls (or sandy muds) of thickness $h = 100\,\mathrm{m}$, and a semi-infinite layer of consolidated sediments. We choose as superficial properties for those marls a porosity of 0.7, a compressional velocity ratio c_p/c_w, with c_w the water sound speed just above the sediment, of 1.013, and a compressional attenuation k_p in dB/m/kHz of 0.102. The evolution of celerity, attenuation and density ρ regarding depth up to h are computed using Hamilton's work. The celerity and density in the consolidated P-Q layer (dots on Fig. 1), comes from the CRUST1.0 model [4]. All the layers are considered fluid (no shear effect). Weighted (Hann's window in time and Hamming's in space) overlapped

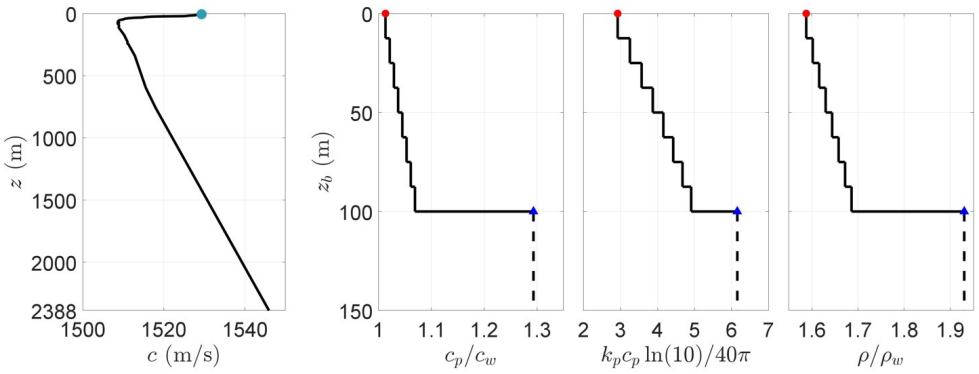

Figure 1: ***Left:*** *Sound-speed volcity profile in water,* ***right:*** *evolution regarding depth of c_p/c_w, normalized k_p (dB/m/kHz), and ρ/ρ_w.*

($50\,\%$) classical beamforming according to time and elevation angle ϕ is performed over the 20 1-s CW emissions. The rapid variation in time of the reverberated field direction of arrival requires short FFT. We chose to perform FFT over 1024 samples (a quarter of the sampling frequency) leading a frequency resolution of $4\,\mathrm{Hz}$. Hence, a 2D cubic interpolation in the (f, ϕ) domain for each temporal bloc is performed to measure RL in dB re $1\,\mu\mathrm{Pa}/\sqrt{\mathrm{Hz}}$ at $215\,\mathrm{Hz}$. Simulation indicates that this operation leads to a bias that do not exceed $+0.25\,\mathrm{dB}$. The 20 outputs of beamforming are then averaged (standard deviations due to ping-to-ping variability around $5\,\mathrm{dB}$) and RL is extracted (white dots on Fig. 2).

2. GABIM IMPLEMENTATION

In the process of implementing GABIM [1], one needs to extract from OASR (one of the software included in the Ocean Acoustics and Seismic Exploration Synthesis (OASES) of H.

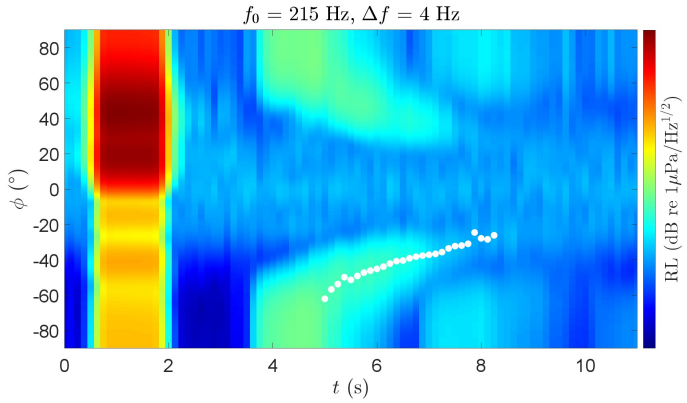

Figure 2: Averaged beamforming output on which the reverberated level is extracted (dots).

Schmidt) the up-going and down-going waves complex amplitudes, A and B respectively, in each layer. We validate this process by successfully comparing our implementation to Fig. 5 of [1] on left part of Fig. 3 that represents the scattering from a very rough rock basement under a smooth sand layer. A second verification consisted in plotting Fig. 11 of [1] with the parameters given in the corrected addendum [5]. The right upper part of Fig. 3 shows strong, unexplained, oscillations for the water-sediment interface roughness and the volume contributions to backscattering strength. A way to reduce the oscillations regarding the water-sediment interface roughness is to consider Eq. (42) of [6] (valid when sediments velocity and density are homogeneous (no gradients)) instead of Eq. (32) of [1]. To reduce the volume contribution oscillations, we have split Eq. (43) of [1] into oscillating-terms proportional to BA^* or to AB^*, with $\cdot^*$ the complex conjugation, and non oscillating-terms proportional to $|A|$ and $|B|$, and only consider the latter for the scattering strength computation. The right lower part of Fig. 3 shows that the oscillations disappeared at the cost of a 5 dB discrepancy in the total scattering strength, for some θ range below 35°. Nevertheless, the overall agreement is reasonable for the use of our implementation of GABIM.

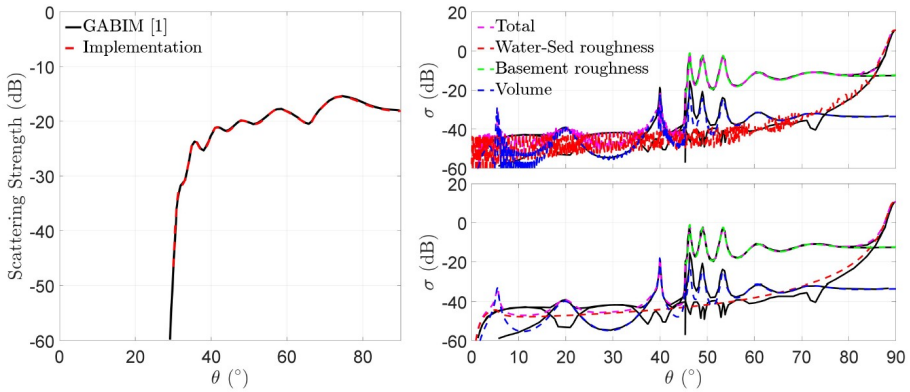

Figure 3: ***Left:*** *Fig. 5 of [1],* ***right:*** *Fig. 1 of [5], without (upper part) and with (lower part) oscillations corrections.*

3. BACKSCATTERING STRENGTH COMPUTATION

The backscattering strength $\sigma(t)$ in dB according to the time t of the RL measurement is computed following:

$$\sigma(t) = \mathrm{RL}(t) - \mathrm{SL} - 10\log_{10}\left(2\pi \int_{R_{\min}(t)}^{R_{\max}(t)} r\mathrm{d}r\mathrm{TL}_g(r)\mathrm{TL}_r(r)D_a(\phi(r),\theta_m(t))\right), \quad (1)$$

where RL is the reverberated level extracted from Fig. 2, SL the source level at 215 Hz in dB re $1\,\mu$Pa/$\sqrt{\text{Hz}}$ @1 m, TL_g and TL_r the transmission losses (re 1 m) from the source to the ensonified area and from the area to the antenna, respectively, and D_a the antenna directivity pattern. $R_{\min}$ and $R_{\max}$ correspond to the inferior and superior radial integration limits, computed numerically with a ray-tracing code, defined such that the go and return time travel $t_0(r)$ is in between $t - \tau/2$ and $t + \tau/2$ where $\tau = 1$ s the CW pulse duration. As the measure of RL at t is the sum of the contributions from all area elements in between $R_{\min}$ and $R_{\max}$, that have been ensonified under a grazing angle from $\theta_{\min}$ to $\theta_{\max}$, one choose to represent the evolution of σ according to a "mean" grazing angle defined as $\theta_m = 0.5(\theta_{\min} + \theta_{\max})$. In Eq. (1), the antenna directivity pattern is taken into account as followed: while pointing in the θ_m direction, the contribution of all area elements is weighted by the directivity pattern evaluated at the elevation angle of arrival ϕ on the antenna, different for each elements. The 2π factor indicates that we already performed the azimuthal integration allowed by the quasi-monostatic configuration of the trial. Finally, all the terms inside the integral in Eq. (1) are expressed on a linear scale.

As the source is immersed near the sea-surface ($\approx$ 7 m) and the emitted wave-length is close ($\approx$ 7.1 m), one needs to be careful when computing the incident pressure field (or TL_g in Eq. (1)) on the ensonified areas. In such configuration, the summation of the complex pressure field (intensity plus phase) associated with each ray should be favored. This produces an emission directivity pattern ("Llyod mirror") that has a strong influence on the incident pressure field at the sea-floor (see left image of Fig. 4). In contrast, the incoherent summation of intensity only produces a incident pressure field on the sea-floor that decays slowly with respect to r (right image of Fig. 4). The computation of σ following Eq. (1) is realized with both $\mathrm{TL}_g^{(C)}$ and

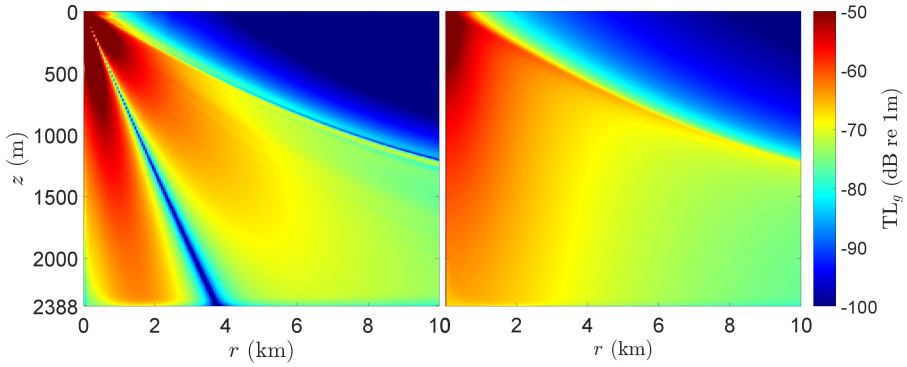

Figure 4: ***Left:*** *Coherent pressure field,* ***right:*** *incoherent pressure field.*

$\mathrm{TL}_g^{(I)}$, the transmission losses from the source to the sea-floor obtained from the coherent and incoherent summation, respectively. The scattering strengths are displayed, along with the measurements of [2], against θ_m on Fig. 5 (left part). Using $\mathrm{TL}_g^{(C)}$ for the calculation of σ produces a strong bump for $\theta_m \approx 32° \approx \tan^{-1}(2388/3800)$ due to the zero in the emission directivity

pattern, whereas σ based on $\mathrm{TL}_g^{(I)}$ is in a better qualitative agreement with past observations. This bump is typically an artifact arising from the classical assumption in Eq. (1) the scattering process occurs at the water-sediment interface [2]. The incident field on the sediment volume and on the sub-bottom interface should be considered instead. Regarding σ based on $\mathrm{TL}_g^{(I)}$, if the SL was not high enough to address the grazing angles lower than $25°$, a strong decrease appears from $\theta_m \approx 33°$. The right part of Fig. 5 represents the three contributions to the total scattering strength issued from our implementation of GABIM calculated with the geoacoustic model described by Fig. 1 (the basement being the sub-bottom interface between the unconsolidated and the consolidated sediments) and the interpolation of the parameters σ_2 and w_2 found in Table I of [1] with respect to $\nu_p = c_p/c_w$. The parameters σ_2 and w_2 are the dimensionless isotropic volume backscattering cross section and the spectral strength of interface roughness, respectively. One sees that both the contributions to σ of the water-sediment and the sub-bottom interfaces are negligible compared to the volume one. The left part of Fig. 6 shows that our im-

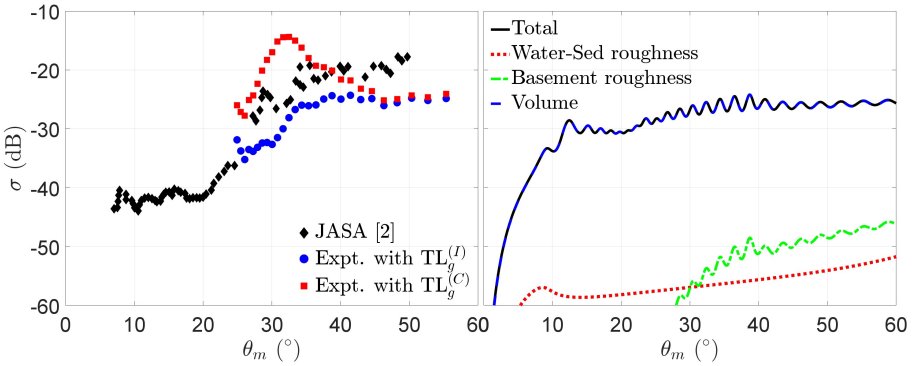

Figure 5: ***Left:*** *Measured backscattering strengths,* ***right:*** *detailed scattering contributions issued from our implementation of GABIM.*

plementation of GABIM, computed with σ_2^G issued from Table I of [1] decently agrees with the measured backscattering strength. A better agreement is achievable if one plays with the evolution of σ_2 w.r.t. z_b. The right part of Fig. 6 shows the volume contribution computed with $\sigma_2(z_b) = \sigma_2^G/4$ for $z_b < 75\,\mathrm{m}$ and $\sigma_2(z_b) = 2\sigma_2^G$ for $z_b \geq 75$. Such an evolution of σ_2 could physically account for upper sediment layers (from $0 < z_b < 75$ meters) less inhomogeneous and deeper layers ($z_b \geq 75$ meters) including turbidites for example. Hence, the volume contribution to backscattering strength of GABIM may account for the strong decrease of σ w.r.t. θ. The significant variation of the modeled σ regarding σ_2 shows that a good agreement between measures and modeling requires a rightful geoacoustic model and a judicious choice for the parameters describing random variations. Nevertheless, the decent agreement obtained on Fig. 6 between measures and modeling based on a first-guess geoacoustic model (Fig. 1) and on the typical values given by Table I of [1] make us confident about using our implementation of GABIM for estimating reverberation level for very low frequency active sonar performances.

4. CONCLUSION

In this paper, a bottom backscattering strength measurement on several 1-s CW at $215\,\mathrm{Hz}$ in the western Mediterranean Sea is described. The acoustic source (immersed at $\approx 7\,\mathrm{m}$) being in the vicinity of the sea-surface, coherent and incoherent incident pressure fields may be

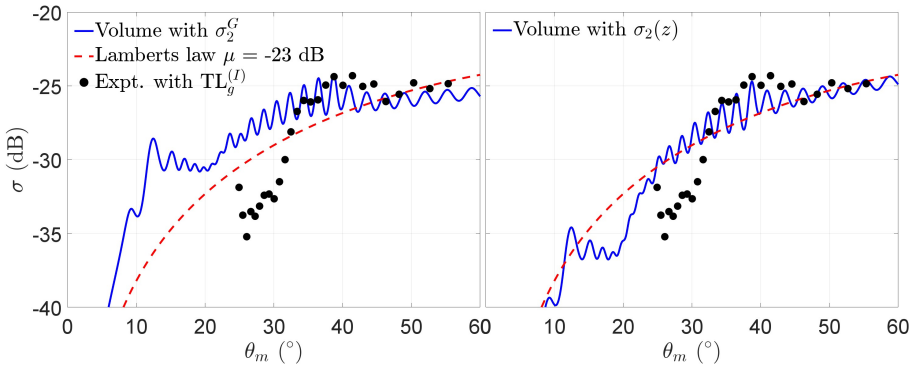

Figure 6: Scattering strength issued from our implementation of GABIM for ***left:*** $\sigma_2 = \sigma_2^G$, ***right:*** $\sigma_2(z)$, *compared to the measured backscattering.*

considered for the measure of σ. While the zero in the emission beam pattern ("Llyod mirror effect") of the coherent field induces a strong bump (artifact according to [2]) in the backscattering strength, the computation of σ upon the incoherent field is in good qualitative agreement with past measurement. Our implementation of GABIM [1], used with a first-guess geoacoustic model and the default parameters describing random variations provided in [1], shows that the isotropic volume inhomogeneities are the main contribution to the overall backscattering strength and allowed decent agreement with the measurements. Moreover, a variation of the volume backscattering strength w.r.t. depth (e.g. to account for deep turbidites layers) may retrieve the strong decrease of the total backscattering strength w.r.t. to the grazing angle.

REFERENCES

[1] D. R. Jackson, R. I. Odom, M. I. Boyd, A. N. Ivakin : "A Geoacoustic Bottom Interaction Model (GABIM)", *IEEE J. Oceanic Eng.* **35**, 603-617, **(2010)**.

[2] C. W. Holland, P. Neumann : "Sub-bottom scattering: A modeling approach", *J. Acoust. Soc. Am.* **104**, 1363-1373, **(1998)**.

[3] M. Bellucci, et al. : "A comprehensive and updated compilation of the seismic stratigraphy markers in the Western Mediterranean Sea", *SEANOE*, **(2021)**.

[4] G. Laske, G. Masters, Z. Ma, M. Pasyanos : "Update on CRUST1.0 - A 1-degree Global Model of Earth's Crust", *Geophys. Res. Abstracts* **15**, Abstract EGU2013-2658, **(2013)**.

[5] D. R. Jackson, R. I. Odom, M. I. Boyd, A. N. Ivakin : "Corrections to "A Geoacoustic Bottom Interaction Model (GABIM)"", *IEEE J. Oceanic Eng.* **36**, 373, **(2011)**.

[6] J. E. Moe, D. R. Jackson : "First-order perturbation solution for rough surface scattering cross section including the effects of gradients", *J. Acoust. Soc. Am.* **96**, 1748-1754, **(1994)**.